

# Off-resonant double-resonance optical-pumping spectra and their application in a multiphoton cesium magneto-optical trap\*

Yang Bao-Dong(杨保东)<sup>a)b)</sup>, He Jun(何 军)<sup>a)</sup>, and Wang Jun-Min(王军民)<sup>a)†</sup>

<sup>a)</sup>State Key Laboratory of Quantum Optics and Quantum Optics Devices, and Institute of Opto-Electronics, Shanxi University, Taiyuan 030006, China

<sup>b)</sup>College of Physics and Electronic Engineering, Shanxi University, Taiyuan 030006, China

(Received 6 November 2013; revised manuscript received 28 December 2013; published online 25 March 2014)

We present an investigation of double-resonance optical pumping (DROP) spectra under the condition of single-photon frequency detuning based on a cesium  $6S_{1/2}$ – $6P_{3/2}$ – $8S_{1/2}$  ladder-type system with a room-temperature vapor cell. Two DROP peaks are found, and their origins are explored. One peak has a narrow linewidth due to the atomic coherence for a counterpropagating configuration; the other peak has a broad linewidth, owing to the spontaneous decay for a copropagating configuration. This kind of off-resonant DROP spectrum can be used to control and offset-lock a laser frequency to a transition between excited states. We apply this technique to a multiphoton cesium magneto-optical trap, which can efficiently trap atoms on both red and blue sides of the two-photon resonance.

**Keywords:** double-resonance optical pumping, electromagnetically induced transparency, two-color laser cooling, laser spectroscopy

**PACS:** 42.50.Gy, 32.80.Xx, 37.10.De, 42.62.Fi

**DOI:** 10.1088/1674-1056/23/5/054205

## 1. Introduction

Doppler-free spectroscopy between excited states has been investigated and widely used in applications such as frequency references in optical communication, high-resolution spectroscopy, and laser cooling/trapping of atoms. A new method for excited states spectroscopy – double-resonance optical pumping (DROP) spectroscopy – is based on the interaction of atoms with two optical fields resonantly tuned to the two transitions that share a common intermediate excited state in a ladder-type atomic system.<sup>[1,2]</sup> Unlike the sophisticated optical-optical double resonance (OODR) technique, which works by detecting the atomic population in the intermediate excited state,<sup>[3,4]</sup> DROP detects the variation of the atomic population in the ground state. Consequently, it can remarkably improve the signal-to-noise ratio (SNR) of the excited spectrum for an atomic system whose lower transition has a very large spontaneous decay rate. DROP spectra have been studied and have many applications, such as stabilizing a laser's frequency to an atomic excited state transition, precise measurement of the hyperfine splitting of atomic excited states, determination of the hyperfine structure constant, and so on.<sup>[5–10]</sup> However, the above investigations have all been focused on the resonant DROP spectra. DROP spectra under the off-resonant (single-photon frequency detuning) condition are seldom studied.<sup>[11]</sup>

In this paper, we investigate the off-resonant DROP spec-

tra based on a cesium  $6S_{1/2}$ – $6P_{3/2}$ – $8S_{1/2}$  ladder-type system with an atomic vapor cell near room temperature. When the lower laser is detuned from the lower transition, the upper laser is oppositely detuned from the upper transition for the requirement of zero two-photon detuning. This provides us with an effective method to offset-lock the upper laser by using the off-resonant DROP spectra, and to conveniently control the single-photon detuning of the upper laser by adjusting the single-photon detuning of the lower laser. This offset-locking scheme has been used in laser frequency stabilization, imaging of cold atoms without a background, and four-wave mixing experiments.<sup>[12–16]</sup> Here, we apply this offset-locking scheme in a frequency system for a new-type cesium magneto-optical trap (MOT) configuration, the multiphoton cesium MOT.<sup>[17]</sup> The multiphoton MOT cools and traps neutral atoms partially by employing a radiation force due to the transition between atomic excited states, instead of the one due to the single-photon transition between the ground state and the excited state in the conventional cesium MOT.<sup>[18–20]</sup> It allows completely background-free detection of laser-induced-fluorescence (LIF) photons of the trapped cold atoms in the MOT.<sup>[13]</sup> It is also possible to directly generate a twin beam (or correlated photon pairs) in this multiphoton MOT based on a diamond-configuration four-wave mixing process.<sup>[15,16]</sup>

This paper is organized as follows. In Section 2, we present the experimental setup of the off-resonant DROP spec-

\*Project supported by the National Basic Research Program of China (Grant No. 2012CB921601), the National Natural Science Foundation of China (Grant Nos. 11104172, 11274213, 61205215, and 61227902), the Project for Excellent Research Teams of the National Natural Science Foundation of China (Grant No. 61121064), the Research Project for Returned Abroad Scholars from Universities of Shanxi Province, China (Grant No. 2012-015), and the Program for Science and Technology Star of Taiyuan, Shanxi, China (Grant No. 12024707).

†Corresponding author. E-mail: [wwjjmm@sxu.edu.cn](mailto:wwjjmm@sxu.edu.cn)

troscopy, and use it for offset-locking of the upper laser operated at the excited states transition for laser cooling in the multiphoton cesium MOT. In Section 3, we discuss the experimental results. Section 3 is divided into two subsections, dealing with the off-resonant DROP spectra and the multiphoton cesium MOT, respectively. Finally, we draw a conclusion.

## 2. Experimental setup

Figure 1 shows the schematic diagrams of the experimental setup for the off-resonant cesium DROP spectroscopy and the multiphoton cesium MOT. In the DROP experiments, the lower laser as the probe laser is provided by an external cavity diode laser (ECDL1), which is locked to the cesium

$6S_{1/2}F = 4$  (state  $|g\rangle$ )– $6P_{3/2}F' = 5$  (state  $|e\rangle$ ) cycling transition by using polarization spectroscopy. The probe laser frequency detuning  $\Delta_p$  from the cesium  $|g\rangle$ – $|e\rangle$  transition can be changed by an acousto-optical modulator (AOM3). The upper laser as the coupling laser is supplied by another external cavity diode laser (ECDL3), which is scanning over the  $6P_{3/2}F' = 5$  (state  $|e\rangle$ )– $8S_{1/2}F'' = 4$  (state  $|e''\rangle$ ) transition. The counterpropagating probe and coupling laser beams overlap in a 5-cm-long cesium vapor cell near room temperature by a dichroic filter (DF). The DROP spectra detected by a photodiode (PD) are recorded on a digital storage oscilloscope (not shown in Fig. 1), and the frequency is calibrated using a confocal Fabry–Perot cavity (also not shown in Fig. 1) with a finesse of  $\sim 100$  and a free spectral range of 735 MHz.

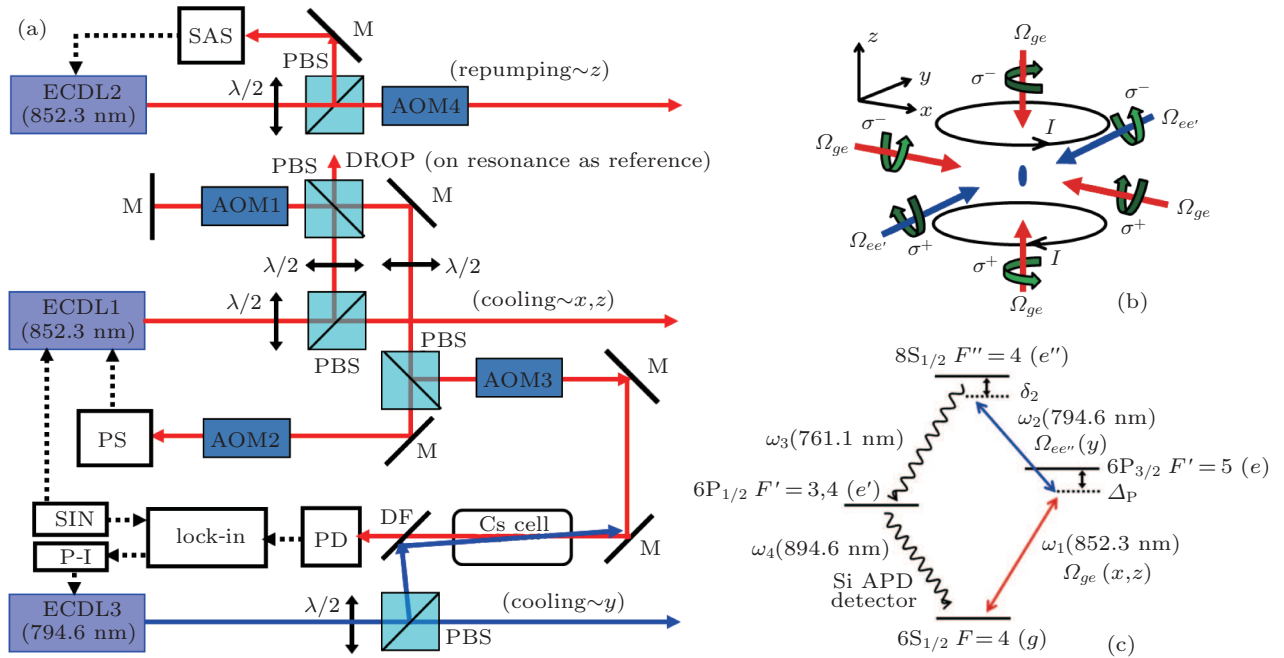


**Fig. 1.** (color online) Schematic diagrams of (a) the setup for the off-resonant DROP spectroscopy and (b) the multiphoton cesium MOT. (c) Simplified level diagram and the related hyperfine levels. Keys to the figure: ECDL: external-cavity diode laser; SAS: saturated-absorption spectroscopy; PS: polarization spectroscopy; AOM: acousto-optical modulator; lock-in: lock-in amplifier; P-I: proportion and integration amplifier; SIN: sine-wave signal generator; DF: dichroic filter; M: mirror; PBS: polarization beam splitting cube;  $\lambda/2$ : half-wave plate; PD: photodiode;  $\sigma^+$ :  $\sigma^+$  circular polarization;  $\sigma^-$ :  $\sigma^-$  circular polarization;  $I$ : the current of anti-Helmholtz coils; APD: avalanche photodiode.

The multiphoton MOT employs a radiation force due to the  $|e\rangle$ – $|e''\rangle$  transition along one axis of the MOT (here the  $y$  axis, see Figs. 1(b) and 1(c)) and due to the  $|g\rangle$ – $|e\rangle$  transition along the other two axes (here the  $x$  and  $z$  axes). This is clearly different from the conventional MOT, which cools and traps atoms using the radiation force completely due to the  $|g\rangle$ – $|e\rangle$  transition along all  $x$ ,  $y$ , and  $z$  axes. The 852.3 nm cooling/trapping beams (Rabi frequency  $\Omega_{ge}$ ) along the  $x$  and  $z$  axes are provided by the ECDL1 with frequency detuning  $\Delta_p = -10$  MHz from the  $|g\rangle$ – $|e\rangle$  transition. The 794.6 nm cooling/trapping beams (Rabi frequency  $\Omega_{ee''}$ ) along the  $y$  axis

is provided by the ECDL3 with frequency detuning  $\Delta_c$  from the  $|e\rangle$ – $|e''\rangle$  transition, so the two-photon frequency detuning is  $\delta_2 = -10$  MHz +  $\Delta_c$  for the cascade  $|g\rangle$ – $|e\rangle$ – $|e''\rangle$  two-photon excitation. The helicities of the 794.6 nm cooling laser beams for the 6P–8S transition are opposite to those for the 6S–6P transition in the conventional MOT. The ECDL3 is locked using the off-resonant DROP spectra, the detailed locking technique has been presented in our previous work.<sup>[2]</sup> The ECDL2 serves as the repumping laser, and is locked to the cesium  $F = 3$  to  $F' = 4$  transition by using the saturated absorption spectroscopic (SAS) locking scheme.

### 3. Experimental results and discussion

#### 3.1. Off-resonant double-resonance optical-pumping spectra

For the cesium  $6S_{1/2}$ - $6P_{3/2}$ - $8S_{1/2}$  ladder-type system, the DROP detects the variation of the atomic population in the ground state  $|g\rangle$  due to the  $|g\rangle$ - $|e\rangle$ - $|e''\rangle$  cascade two-photon excitation and thereafter due to the cascade spontaneous decay to another hyperfine fold  $F = 3$  in the ground state. When the probe laser is locked to the  $|g\rangle$ - $|e\rangle$  transition, part of the zero-velocity atoms will be populated on state  $|e\rangle$ . When the upper laser is scanned over the  $|e\rangle$ - $|e''\rangle$  transition, part of the atoms on state  $|e\rangle$  are further excited to state  $|e''\rangle$ . Finally, some zero-velocity atoms on state  $|e''\rangle$  will decay to another hyperfine fold  $F = 3$  in the ground state via  $8S_{1/2}F'' = 4-6P_{3/2}F' = 3(4)-6S_{1/2}F = 3$  and  $8S_{1/2}F'' = 4-7P_{1/2}(7P_{3/2})-6S_{1/2}F = 3$  cascade decay channels (some hyperfine levels are not shown in Fig. 1(c)), which will decrease the absorption of the probe beam, forming the DROP spectra. Now, the observed DROP spectrum corresponds to the  $|e\rangle$ - $|e''\rangle$  resonant transition.<sup>[1,2]</sup>

When the lower laser has a single-photon detuning  $\Delta_p$  to the  $|g\rangle$ - $|e\rangle$  transition, for example,  $\Delta_p = 120$  MHz, we often see double DROP peaks for a counter-propagating (CTP) configuration (the lower trace in Fig. 2(a)) and a co-propagating (CP) configuration (the upper trace in Fig. 2(a)). The related experimental parameters are as follows: the diameter and the power of the probe laser are  $\sim 2.0$  mm and  $\sim 0.3$  mW, and those of the coupling laser are  $\sim 2.2$  mm and  $\sim 6$  mW, respectively. Similar experimental results have been reported in Ref. [11]. Note that the two peaks are symmetrically situated on the two sides of the double-resonance point ( $\Delta_p = \Delta_c = 0$ ). In the case of the CTP configuration, the left peak can be easily understood: when  $\Delta_p = 120$  MHz, a group of atoms on state  $|g\rangle$  with certain velocity  $V$  along the probe laser direction (the Doppler shift  $\Delta f_p = -Vf_p/c = -V/\lambda_p = -120$  MHz, here  $f_p$  is probe laser's frequency,  $c$  is the speed of light in vacuum,  $\lambda_p = c/f_p$  is the probe laser's wavelength) will be populated on state  $|e\rangle$ , and these atoms have a Doppler shift  $\Delta f_c = Vf_c/c = V/\lambda_c = (\lambda_p/\lambda_c)\Delta f_p \approx +129$  MHz for the upper laser, so this peak will appear when the upper laser is scanned to  $\Delta_c = -129$  MHz. We ascribe the right DROP peak of the lower trace in Fig. 2(a) to a coupling beam's reflection on the surface of a cesium vapor cell, which simultaneously forms a CP configuration with the probe beam as shown in Fig. 2(b). Because the intensity of the reflection beam is much weaker, this yields that the right peak is weak.

In the case of the CP configuration, as shown in Fig. 2(c), the double peaks are explained by similar reasons as those above. In the upper trace in Fig. 2(a), we can clearly see that the left peak results from the coupling beam's reflection

on the surface of the cesium vapor cell (simultaneously forming a CTP configuration with the probe beam, as shown in Fig. 2(c)), and it has a narrow linewidth compared with the right peak for the CP configuration. This happens because the electromagnetically-induced transparency (EIT) exists for the counterpropagating probe and the coupling beams, which suppresses the linewidth of the DROP spectrum,<sup>[21]</sup> and because the intensity of the reflection beam is much weaker, which yields the weak left peak. However, for the CP configuration, the EIT is almost submerged by the Doppler effect for the ladder-type atomic system in a room temperature vapor cell.<sup>[22-25]</sup> Thus, the right peak for the copropagating probe and the coupling beams is mainly due to the DROP process accompanied with the spontaneous emission, and it has a broad linewidth.

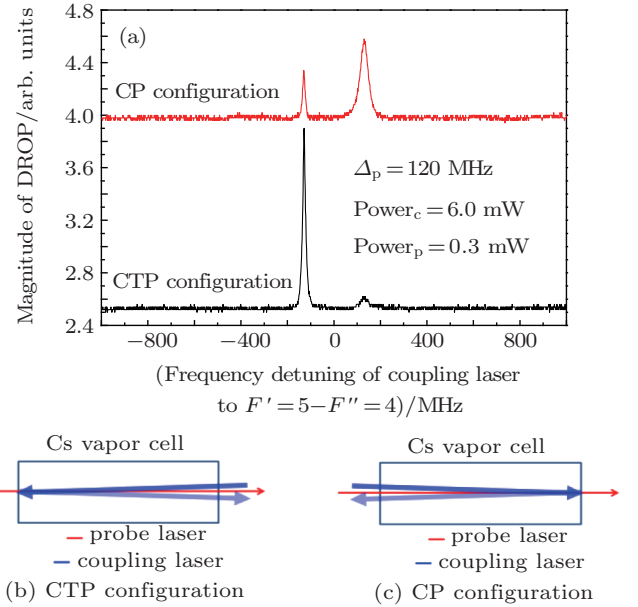


**Fig. 2.** (color online) Off-resonant DROP and their laser beam's arrangements: (a) off-resonant DROP for CTP and CP configurations; (b) laser beams for CTP configuration in cesium vapor cell; (c) laser beams for CP configuration in cesium vapor cell.

When the probe laser has a single-photon detuning  $\Delta_p = -30$  MHz, we demonstrate the off-resonant DROP spectra for CP and CTP configurations with different angles (from  $0^\circ$  to  $7.6^\circ$ ) between the coupling laser beam and the axis of the vapor cell, as shown in Fig. 3. When the angle is increased, the peaks due to the reflection of cesium vapor cell's surface become weaker and cannot even be seen. This happens because the overlap region between the reflection coupling beam and the probe beam is becoming smaller (the number of atoms inside this region is also getting smaller). However, the double peaks keep the same frequency intervals. Thus, the above phenomena directly prove that these small peaks come from the reflection of the coupling beam on the cesium vapor cell's surface.

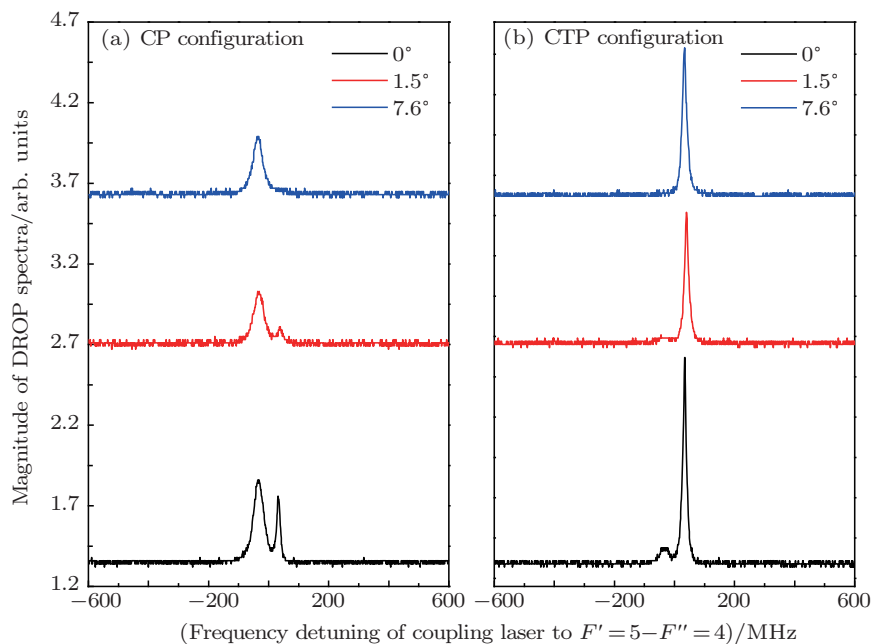


**Fig. 3.** (color online) Off-resonant DROD spectra for (a) CP and (b) CTP configurations at the different angles between the coupling laser beam and the axis of the vapor cell.

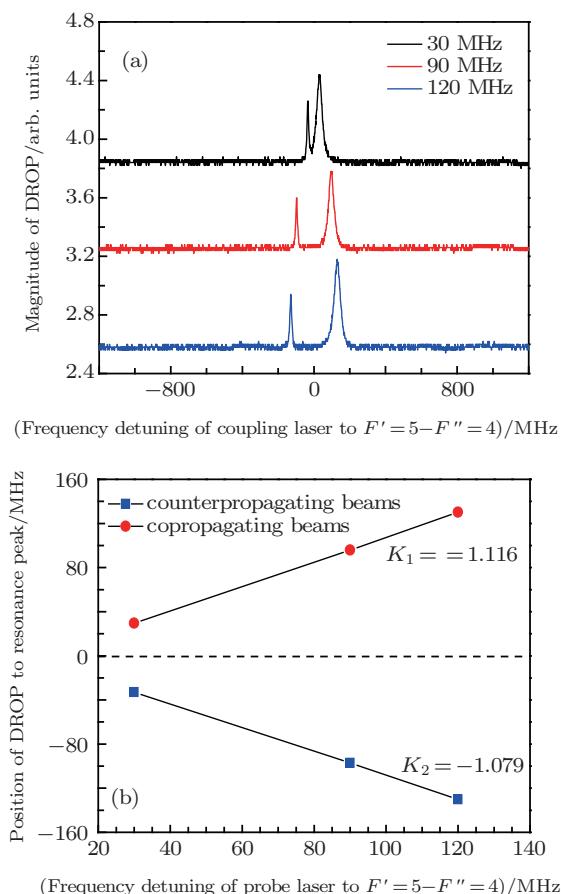


**Fig. 4.** (color online) (a) Off-resonant DROD spectra for copropagating (CP) configuration at different probe laser's frequency detunings. (b) The dependence of the frequency span between the left (right) peak and the double-resonance point ( $\Delta_p = \Delta_c = 0$ ) upon the probe laser's frequency detuning for CTP (CP) configurations, as shown in the lower (upper) trace.

Figure 4(a) shows the off-resonant DROD spectra in the

cases of  $\Delta_p = +30$  MHz,  $+90$  MHz,  $+120$  MHz for the CP configuration. The dependence of the frequency intervals between the left (right) peaks and the double-resonance point ( $\Delta_p = \Delta_c = 0$ ) upon single-photon detuning  $\Delta_p$  is shown as the lower (upper) data points in Fig. 4(b) for the CTP (CP) configurations. The relevant slope of the upper (lower) data points is  $K_1 = 1.116$  ( $K_2 = -1.079$ ) from the linear fitting, which should be in accordance with the value  $\lambda_p/\lambda_c = 852.3/794.6 = 1.073$  for the wavelength mismatch between the probe and the coupling lasers.<sup>[25,26]</sup> Thus, if we know  $\Delta_p$ , we can obtain  $\Delta_c = \Delta_p (\lambda_p/\lambda_c)$  of these peaks relative to the double-resonance point, and further obtain the two-photon detuning  $\delta_2$  in the multiphoton cesium MOT experiment when the upper laser is offset locked via the off-resonant DROD spectrum.

### 3.2. Application of the off-resonant DROD spectra for multiphoton cesium MOT

In our multiphoton cesium MOT experiment, the counterpropagating 794.6 nm cooling/trapping laser beams along the  $y$  axis with a diameter of  $\sim 2.2$  mm is provided by ECDL3, which is offset locked to the  $|e\rangle - |e''\rangle$  transition using the off-resonant DROD spectrum in the case of the CTP configuration (for higher SNR and narrower linewidth compared those in the CP configuration). Its single-photon detuning  $\Delta_c$  can be conveniently controlled by AOM3. The detailed locking technique can be found in our previous work.<sup>[2]</sup> Typical experimental parameters of our multiphoton cesium MOT are as follows: the power of the 852.3 nm cooling/trapping beams

with a diameter of  $\sim 2.2$  mm along the  $x$  and  $z$  axes is up to  $\sim 3.4$  mW, its single-photon detuning from the  $|g\rangle\text{--}|e\rangle$  transition is  $\Delta_p = -10$  MHz; the power of the 794.6 nm cooling/trapping beams along the  $y$  axis is  $\sim 8.6$  mW, its two-photon detuning is  $\delta_2 = -12.1$  MHz; the power of the repumping laser beams with a diameter of  $\sim 2.2$  mm along the  $z$  axis is  $\sim 3.6$  mW; and the gradient of the quadruple magnetic field along the  $z$  axis generated by the anti-Helmholtz coils is about 20 Gauss/cm.

We plot the peak fluorescence intensity of the cold atom cloud versus the two-photon detuning  $\delta_2$  in Fig. 5, which clearly shows that the multiphoton cesium MOT can efficiently trap atoms with both red and blue two-photon detuning  $\delta_2$ . With the red two-photon detuning, the cooling/trapping mechanism can be understood using a two-photon Doppler cooling picture, which is similar to the conventional MOT. With the blue two-photon detuning, the cooling/trapping mechanism may be explained using the multiphoton polarization gradient cooling.<sup>[17]</sup> The above experimental results are very different from the conventional 852.3 nm cesium MOT, which can only trap atoms at red detuning.

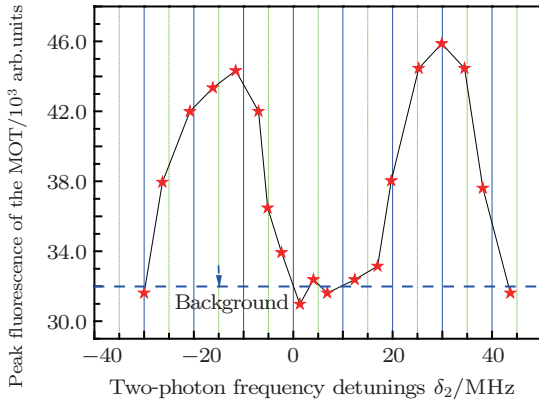


**Fig. 5.** (color online) Peak fluorescence of cold atom cloud versus the two-photon frequency detuning  $\delta_2$ . The solid lines are only used to guide the eyes.

Note that the trapped atoms will be populated on the state  $8S_{1/2}F'' = 4$ , and then emit fluorescence photons at 761.1 nm and 894.6 nm via the intermediate state  $6P_{1/2}$  in the two-photon cooling process of the multiphoton MOT, as shown in Fig. 1(c). The detected fluorescence photons with wavelength 761.1 nm or 894.6 nm can be easily separated from the background 852.3 nm photons from the cooling and the repumping laser beams with a high-suppress-ratio 761 nm or 895 nm interference filter in front of the detector. So we can realize the background-free fluorescence detection of cold atoms,<sup>[13]</sup> which is helpful for weak signal detection (such as a single atom). In order to apply the multiphoton MOT to single atom experiments, we also investigate the dependence of the loading

rate of the multiphoton MOT on the quadruple magnetic gradient. When ignoring the trap loss due to cold collisions in the MOT, the total number  $N(t)$  of cold atoms in the MOT is given by the solution to a simple rate equation  $dN/dt = R_L - N/\tau$ . By assuming  $N(t = 0) = 0$ , the loading rate equation can be written as<sup>[19]</sup>

$$N(t) = R_L \tau [1 - \exp(-t/\tau)], \quad (1)$$

where  $R_L$  is the loading rate, and  $\tau$  is the lifetime, which often depends on the background vacuum pressure. The fluorescence rate  $f$  from the detector is proportional to the numbers  $N$  of the trapped atoms,  $f/N = C$ , where  $C$  is a constant, which is related with the fluorescence photon collection efficiency of the detector, frequency detuning, and the intensity of the cooling laser.<sup>[27]</sup> So, we can obtain the fluorescence rate  $f(t)$  as

$$f(t) = CN(t) = CR_L \tau [1 - \exp(-t/\tau)]. \quad (2)$$

When turning on the multiphoton MOT, the loading curves are obtained by recording the fluorescence of cold atoms using an APD worked in the photon-counting mode (time bin: 50 ms). Figure 6 shows the loading curves for different quadruple magnetic gradients. The experimental data are fitted with Eq. (2), and the parameters  $\tau$  and  $CR_L$  are given. For different quadruple magnetic gradients, the lifetime is approximately the same,  $\tau = 0.32 \pm 0.05$  s. According to the measured lifetime  $\tau$ , our background vacuum pressure is estimated to be  $2.0 \times 10^{-8}$  Torr. The tendency of  $CR_L$  versus quadruple magnetic gradient is plotted in Fig. 7, and the experimental error of 10% is from the fluctuation of the number of cold atoms in the multiphoton MOT. With the increase of the quadruple magnetic gradient ( $> 40$  Gauss/cm), the loading rate rapidly decreases. Haubrich *et al.* gave a simplified analytic model for atom loading in a large-magnetic-field gradient MOT, the loading rate is sensitive to the magnetic gradient<sup>[28,29]</sup>

$$R_L \propto (dB/dz)^{-14/3}. \quad (3)$$

The dependence of loading rates  $CR_L$  on the quadruple magnetic gradient is fitted by formula (3), as shown in Fig. 7, and the experimental data are in agreement with the theoretical prediction. This is helpful for our realization of single-atom multiphoton MOTs and investigation of the statistical characteristics of the fluorescence photons.<sup>[30]</sup>

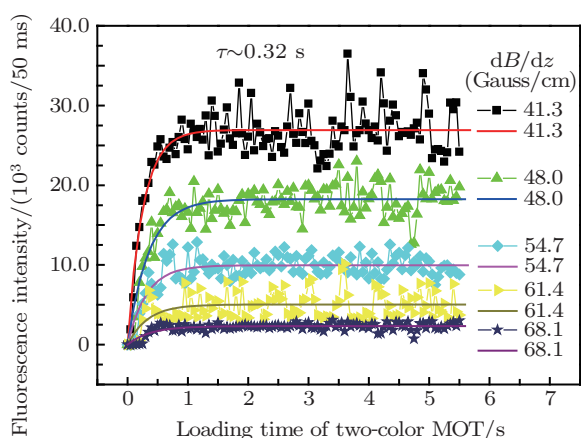


**Fig. 6.** (color online) Loading curves of multiphoton MOTs for different quadruple magnetic gradients. The solid lines represent the theoretical fitting results.

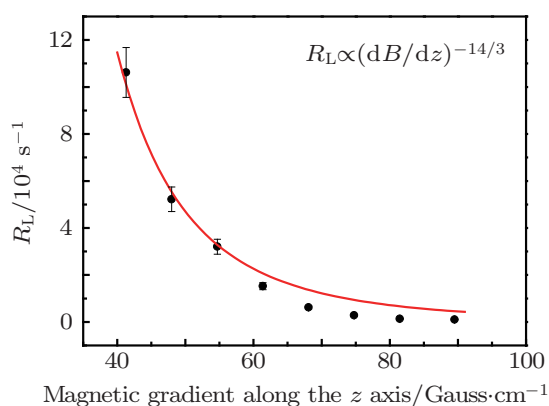


**Fig. 7.** (color online) Dependence of loading rate  $CR_L$  on the quadruple magnetic gradient. The solid circles are experimental data with error bars of 10%; the solid line represents the theoretical prediction.

In addition, in this multiphoton cesium MOT it is possible to directly generate a twin beam (or correlated photon pairs) at 761.1 nm and 894.6 nm based on the diamond-level structure four-wave mixing process as shown in Fig. 1(c),<sup>[15,16,31,32]</sup> in which the two cooling lasers (852.3 nm and 794.6 nm) again serve as the two pump lasers in the four-wave mixing process. This method can be extended to the Rubidium atom multiphoton MOT. In this case one photon, with wavelength 780 nm, is suited for mapping to a long-lived atomic quantum memory, and the other photon, with wavelength 1.53  $\mu\text{m}$ , is ideal for long-distance quantum communication.

#### 4. Conclusion

We have investigated the off-resonant DROP spectra with a room-temperature cesium vapor cell and have explored the origins of the double DROP peaks in experiment. The off-resonant DROP spectra can be used to conveniently control the single-photon frequency detuning of the upper laser by changing the single-photon detuning of the lower laser, which couples the ground state and the shared intermediate excited state.

This provides us with an effective method for offset-locking a laser to the transition between excited states using an off-resonant DROP spectrum. We have applied this technique to a multiphoton cesium MOT, measured the dependence of the loading rate on the quadruple magnetic gradient, and briefly discussed a proposal of the direct generation of a twin beam in cold atoms from a multiphoton MOT.

#### References

- [1] Moon H S, Lee W K, Lee L and Kim J B 2004 *Appl. Phys. Lett.* **85** 3965
- [2] Yang B D, Zhao J Y, Zhang T C and Wang J M 2009 *J. Phys. D: Appl. Phys.* **42** 085111
- [3] Sasada H 1992 *IEEE Photon. Tech. Lett.* **4** 1307
- [4] Boucher R, Breton M, Cyr N, Julien C and Tetu M 1992 *IEEE Photon. Technol. Lett.* **4** 327
- [5] Noh H R and Moon H S 2009 *Phys. Rev. A* **80** 022509
- [6] Yang B D, Liang Q B, He J, Zhang T C and Wang J M 2010 *Phys. Rev. A* **81** 043803
- [7] Moon H S, Lee L and Kim J B 2007 *J. Opt. Soc. Am. B* **24** 2157
- [8] Moon H S, Lee L and Kim J B 2008 *Opt. Express* **16** 12163
- [9] Kargapol'tsev S V, Velichansky V L, Yarovitsky A V, Taichenachev A V and Yudin V I 2005 *Quant. Electron.* **35** 591
- [10] Zhao J M, Zhu X B, Zhang L J, Feng Z G, Li C Y and Jia S T 2009 *Opt. Express* **17** 15821
- [11] Chang R Y, Fang W C, He Z S, Ke B C, Chen P N and Tsai C C 2007 *Phys. Rev. A* **76** 053420
- [12] Bell S C, Heywood D M, White J D, Close J D and Scholten R E 2007 *Appl. Phys. Lett.* **90** 171120
- [13] Yang B D, Liang Q B, He J and Wang J M 2012 *Opt. Express* **20** 11944
- [14] Ohadi H, Himsworth M, Xuereb A and Freearge T 2009 *Opt. Express* **17** 23003
- [15] Becerra E, Willis R T, Rolston S L and Orozco L A 2008 *Phys. Rev. A* **78** 013834
- [16] Willis R T, Becerra F E, Orozco L A and Rolston S L 2009 *Phys. Rev. A* **79** 033814
- [17] Wu S, Plisson T, Brown R C, Phillips W D and Porto J V 2009 *Phys. Rev. Lett.* **103** 173003
- [18] Chu S, Hollberg L, Bjorkholm J E, Cable A and Ashkin A 1985 *Phys. Rev. Lett.* **55** 48
- [19] Monroe C, Swann W, Robinson H and Wieman C 1990 *Phys. Rev. Lett.* **65** 1571
- [20] Hu Z and Kimble H J 1994 *Opt. Lett.* **19** 1888
- [21] Yang B D, Gao J, Liang Q B, Wang J, Zhang T C and Wang J M 2011 *Chin. Phys. B* **20** 044202
- [22] Yang H, Yan D, Zhang M, Fang B, Zhang Y and Wu J H 2012 *Chin. Phys. B* **21** 114207
- [23] Gea-Banacloche J, Li Y Q, Jin S Z and Xiao M 1995 *Phys. Rev. A* **51** 576
- [24] Iftiqar S M, Karve G R and Natarajan V 2008 *Phys. Rev. A* **77** 063807
- [25] Yang B D, Gao J, Zhang T C and Wang J M 2011 *Phys. Rev. A* **83** 013818
- [26] Mohapatra A K, Jackson T R and Adams C S 2007 *Phys. Rev. Lett.* **98** 113003
- [27] Marcassa L, Bagnato V, Wang Y, Tsao C and Weiner J 1993 *Phys. Rev. A* **47** 4563
- [28] Haubrich D, Höpe A and Meschede D 1993 *Opt. Commun.* **102** 225
- [29] He J, Yang B D, Cheng Y J, Zhang T C and Wang J M 2011 *Front. Phys.* **6** 262
- [30] Hennrich M, Kuhn A and Rempe G 2005 *Phys. Rev. Lett.* **94** 053604
- [31] Song M and Yoon T H 2011 *Phys. Rev. A* **83** 033814
- [32] Akulshin A M, Orel A A and McLean R J 2012 *J. Phys. B: At. Mol. Opt. Phys.* **45** 015401